Available online at www.sciencedirect.com
ScienceDirect
Trans. Nonferrous Met. Soc. China 27(2017) 789−796
Transactions of Nonferrous Metals Society of China
www.tnmsc.cn

Influence of multi-pass friction stir processing on microstructure and mechanical properties of 7B04-O Al alloy

Yu CHEN[1], Hua DING[1], S. MALOPHEYEV[2], R. KAIBYSHEV[2], Zhi-hui CAI[1], Wen-jing YANG[1]

1. School of Materials Science and Engineering, Northeastern University, Shenyang 110819, China;
2. Laboratory of Mechanical Properties of Nanoscale Materials and Superalloys, Belgorod State University, Belgorod 308015, Russia

Received 21 February 2016; accepted 30 August 2016

Abstract: Three-pass friction stir processing (FSP) with different moving distances of the stirring tool between the two successive passes, 50% diameter of the pin (traditional way) and 50% diameter of the shoulder (novel way), was conducted on 7B04-O Al alloy. The result shows that an improvement in the mechanical properties of the processed zone is accomplished due to grain and second phase particles refinement. The hardness of the multi-pass FSP (M-FSP) sample is about HV 40 higher than that of the base metal. And the tensile strength of the M-FSP specimens is also significantly increased to about 1.4 times that of the base metal. Besides, the weak region of the processed zone is mainly dependent on the moving distance, where it is the previous pass stir zone in the traditional way and the transitional zone in the novel way. Increasing the rotational speed narrows the weak region in the novel way, while it does not in the traditional way.

Key words: friction stir processing; multi-pass; grain refinement; aluminum alloy

1 Introduction

Friction stir processing (FSP) was developed based on the friction stir welding (FSW). The concept of FSP is remarkably simple: a rotating tool is plunged into a fixed workpiece and traverses along the line of interest [1−4]. Since its development, FSP has been applied to refining grains, modifying microstructures and achieving superplasticity [5−7]. However, the narrow processed zone of single-pass FSP is not suitable for practical engineering applications, e.g., a pin diameter of 6 mm only produces a processed zone 6−8 mm in width [8]. The extension of FSP to multi-pass FSP (M-FSP) addresses this issue, and the overlapping of passes can be used to produce bulk-processed materials [9−11]. At present, several researchers have investigated the effect of M-FSP on microstructure and mechanical properties of the aluminum alloys, and M-FSP is often applied in the work-hardened base metal, e.g., as-rolled [12], peak aged [13] and hot extrusion [14] states. Nevertheless, M-FSP in work hardened condition of base metal reduces tool life because of its high resistance to deformation, increasing the cost of production [15]. 7B04 Al alloy is a precipitation-hardened Al−Zn−Mg−Cu aluminum alloy, which has been widely applied to producing aircraft parts due to its light mass and high strength [16,17]. Unfortunately, on account of the high strength of 7B04 Al, the lifetime of the stirring tool becomes short. In order to decrease the cost of production, 7B04-O Al alloy (soft condition, annealed state) can be applied for M-FSP due to its excellent formability and low resistance to deformation.

Besides the initial base metal temper, the distance between axial axes in two successive passes is another important M-FSP parameter, which is defined by l/d, where l is the moving distance of the pin between two successive passes (the moving distance) and d is the diameter of the pin [11]. Generally, the moving distance selected is always not larger than the diameter of the pin (namely, $l/d \leq 1$). In this condition, the materials in the processed zone undergo repeated directly stirring of the pin; however, no researchers have tried to enlarge the moving distance further ($l/d>1$), hence, it is necessary to fulfill the insufficient data at $l/d>1$.

In this work, M-FSP is conducted on 7B04-O Al alloy using two moving distances. In the first case, the moving distance is 50% of the pin diameter ($l/d<1$) and

Corresponding author: Hua DING; Tel: +86-24-83673081; Fax: +86-24-23906316; E-mail: crainy11@126.com
DOI: 10.1016/S1003-6326(17)60090-6

called as traditional way. In the second case, the moving distance is enlarged to 50% of the shoulder diameter (in the present case, D=12.5 mm and d=5 mm, namely l/d>1) and called as novel way. The M-FSP behaviors with different l/d (the moving distance) on the microstructure and mechanical properties of the processed zone are investigated.

2 Experimental

Rolled 7B04 aluminum alloy sheets of 2 mm were applied in this study, and the nominal chemical compositions of this alloy are listed in Table 1. Annealed O-temper was adopted for 7B04 Al plates before FSP. Annealed O-temper comprised of initial heating to 400°, soaking for 1 h, followed by furnace cooling to 150° and air cooling down to ambient temperature. Three-pass M-FSP sheets with different moving distances were performed using an AccuStir 1004 FSW machine with a tool rotational speed of 400 r/min and a tool travel speed of 200 mm/min. The stirring tool was tilted by 2.5° from the sheet normal such that the rear of the tool was lower than the front. The FSP tool consisted of a shoulder with a diameter of 12.5 mm and a M5 cylindrical pin with a length of 1.9 mm. The rotational orientation was counterclockwise. After each pass, the plate was cooled down to room temperature about 5 min to eliminate the effect of accumulative heating, and then the subsequent pass (overlapping by the retreating side) was performed. The moving distance of the pin was 2.5 mm (50% diameter of the pin, l/d=0.5), and 6.25 mm (50% diameter of the shoulder, l/d=1.25). In this work, the FSP direction was denoted as PD, the normal direction was ND, and the traverse direction was TD.

Table 1 Nominal chemical compositions of studied 7B04 aluminum alloy (mass fraction, %)

Zn	Mg	Cu	Mn	Fe	Si	Cr	Al
6.0	2.2	1.6	0.3	0.1	<0.1	0.1−0.25	Bal.

The microstructure of the processed zone was examined in the transversal cross-sections by Olympus DSX 500 optical microscopy (OM), electron backscatter diffraction (EBSD) and transmission electron microscopy (TEM). The samples for OM were ground and polished and then etched using Keller's reagent (190 mL water, 2 mL hydrofluoric acid, 3 mL hydrochloric acid and 5 mL nitric acid). The EBSD analysis was conducted using a FEI Quanta 600 field-emission-gun scanning electron microscope (FEG-SEM) equipped with TSL OIM^{TM} software. The scanning step of EBSD analysis was 0.2 μm, and the scanning area was 2500 μm^2. In the grain-boundary EBSD maps, the low-angle grain boundaries (LAGBs) (2°<θ<15°) and the high-angle grain boundaries (HAGBs) (θ>15°) were depicted as light grey and dark black lines, respectively. The TEM observations were performed by using a Tecnai G^{2}20. Suitable surfaces for EBSD and TEM were obtained by electropolishing in a solution of 25% nitric acid in ethanol at −32 °C and 19.5 V.

The Vickers hardness data were obtained by applying a load of 50 g with a dwell time of 10 s on a Wolpert 402MVD hardness tester with a distance between the neighboring measured points of 0.5 mm. The hardness profiles were obtained along the centerline of the transversal cross-section at the sheet mid-thickness. Room-temperature tensile tests were conducted at a constant crosshead velocity corresponding to an initial strain rate of 1×10^{-3} s^{-1} using an Instron 5882 universal testing machine. For M-FSP, the transverse tensile specimens were cut perpendicular to the PD with a gauge section that was 3 mm-wide and 8 mm-long. And the dimension of the tensile specimens was smaller than the width of the processed zone, which could represent the exact tensile properties of the processed zone. For single-pass FSP, the longitudinal tensile specimens with the same dimension were cut along the FSP centerline only including the stir zone. The upper and lower surfaces of all the tensile specimens were mechanically polished to achieve a uniform thickness and to prevent the surface defects from affecting the tensile properties of the samples. The dimensions of the tensile specimen are indicated in Fig. 1. The cross-section dimensions of the transverse tensile specimen are 3 mm in width and 1.6 mm in thickness.

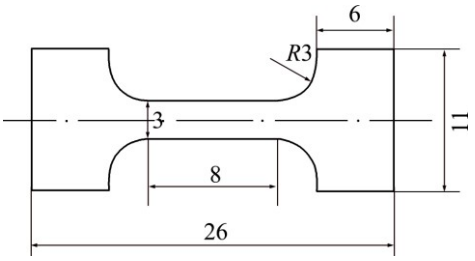

Fig. 1 Dimensions of tensile test specimen (unit: mm)

3 Results and discussion

3.1 Microstructural characteristics of processed zone

Figure 2 shows the low-magnification OM images of the processed zone of the M-FSP samples using different moving distances. No defects such as cavity, tunnel and "zigzag line" are found in the processed zone. For the traditional way (Fig. 2(a)), the whole processed zones are directly stirred by the pin, and stir zones from the 1st to the 3rd pass are labeled as A, B and C. It can be seen that the stir zones of the 2nd and 3rd passes are visible while it is not for the 1st pass, and the exact

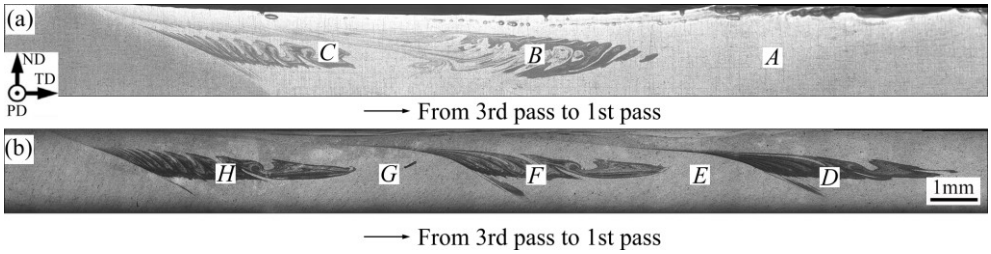

Fig. 2 Low-magnification optical images of transversal cross-section of M-FSP samples using traditional (a) and novel (b) way

reason for this phenomenon is still unclear. Different from the traditional way, the processed zone in the novel way consists of two parts, the stir zone of each pass is distinctly visible and a new transitional zone between the two adjacent FSP passes is found (Fig. 2(b)). The transitional zone locates next to the stir zone and lacks of the directly stirring of the pin due to the large overlapping applied. Likewise, the stir zones are labeled as *D*, *F* and *H* (as the 1st, 2nd and 3rd pass), and the transitional zones are *E* and *G* (between the 1st and 2nd and 2nd and 3rd, respectively).

The grain morphologies in various microstructural regions, i.e., around locations *A*, *B*, *C*, *D*, *E*, *F*, *G* and *H* in Fig. 2, are examined by EBSD technique and the average grain size of these regions is summarized in Table 2. For comparison, the data for the unprocessed base metal and the single-pass FSP sample, prepared with the same FSP tool geometry and parameters, are also included in Table 2. The typical EBSD grain-mapping results in locations *A*, *C*, *F*, *H* and *G* are presented in Fig. 3, comparing with the original banded structure, the evolved microstructure in the processed zone is dominated by completely recrystallized fine and equiaxed grains which are resulted from the severe plastic deformation and thermal exposure during M-FSP. The grain size and the fraction of HAGBs in the processed zone of M-FSP samples are quite similar to those in the stir zone produced by single-pass FSP. Moreover, the variation in the grain size is negligible for M-FSP samples although different moving distances are applied, which indicates that the moving distance of M-FSP does not result in a significant effect on the size of recrystallized grains.

Table 2 Average grain size in base metal and different regions for single-pass and M-FSP samples

Processing condition	Location	Average grain size/μm
3-pass FSP using traditional way	Region *A* (1st pass)	1.8±0.3
	Region *B* (2nd pass)	1.7±0.3
	Region *C* (3rd pass)	1.5±0.1
3-pass FSP using novel way	Region *D* (1st pass)	1.9±0.5
	Region *E* (1st−2nd pass transition)	1.3±0.1
	Region *F* (2nd pass)	1.9±0.3
	Region *G* (2nd−3rd pass transition)	1.4±0.1
	Region *H* (3rd pass)	1.6±0.3
Base metal		Length 200±50 Width 80±30
Single-pass FSP	Stir zone	1.7±0.1

During single-pass and multi-pass FSP in traditional way, the materials in the processed zone are stirred directly by the pin no less than once, undergo severe plastic deformation and thermal exposure, leading to the dynamic recrystallization (DRX) processing and refining the grain [18]. For the novel way, grain refinement in the stir zone is to be expected because of the directly stirring of the pin, while it is of interest that grain refinement occurs in the transitional zone where there is a lack of stirring. Therefore, it is necessary to research the mechanism of grain refinement in the transitional zone.

The textures of the transitional zone *G* (between the 2nd and 3rd passes) before and after conducting the 3rd pass are examined by extracting the orientation data from the EBSD maps, which are presented as (111) pole figures in Fig. 4. For illustrative purpose, the main ideal simple shear components for the face-centered cubic metals are listed for comparison. Before conducting the 3rd pass, the texture intensity in region *G* is relatively strong, the $B/\overline{B}$ {112}⟨110⟩ simple shear orientation is observed, which indicates that the impact of the shear deformation induced by the second pass is significant in region *G*. After conducting the 3rd pass, the texture intensity in region *G* becomes weak and it is similar to that of the stir zone produced by single-pass FSP. The weakened texture suggests the occurrence of DRX [19]. Based on the observation above, it implies that a two-step microstructural evolution occurs in the transitional zone: the material in the transitional zone lacks directly stirring of the pin but flows around the pin due to the effect of the shoulder. During the successive two passes, the material of the transitional zone locates on the retreating side for the previous pass while advancing side for the subsequent pass. On account of the effect of the shoulder, the material is inclined to flow

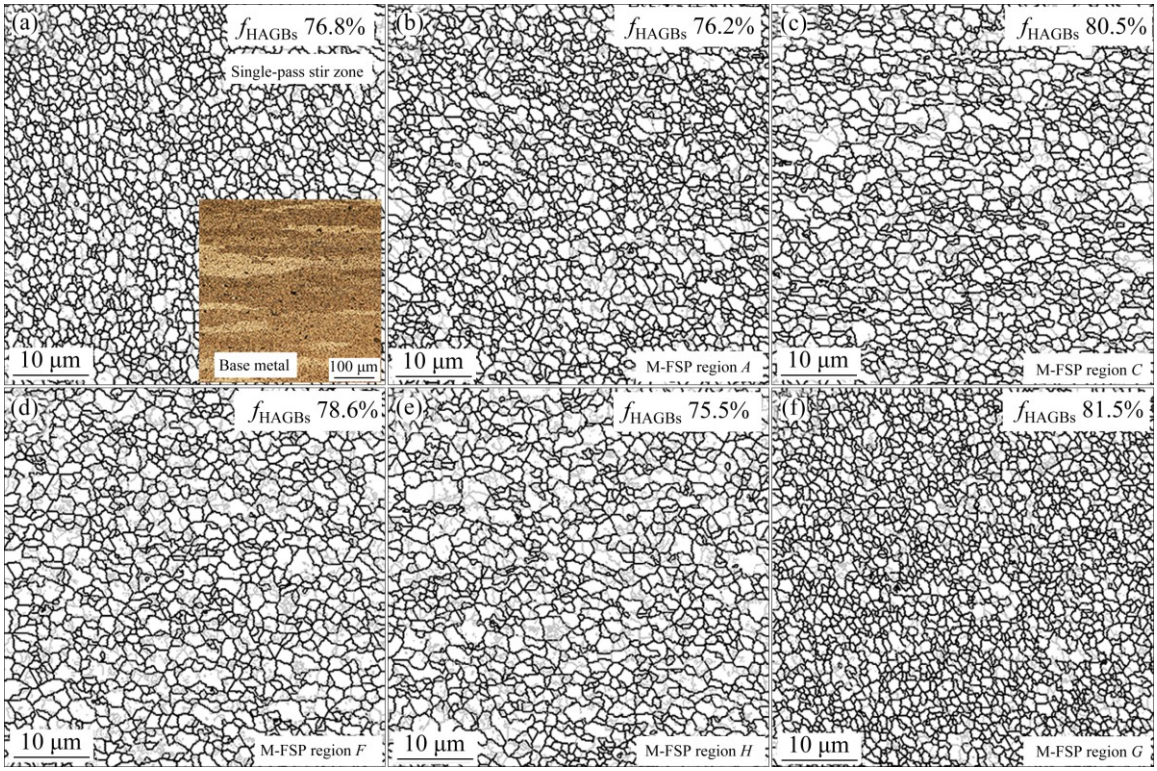

Fig. 3 EBSD grain-boundary maps showing microstructure in different regions of processed zone: (a) Stir zone of single-pass FSP; (b) The first pass stir zone *A*; (c) The third pass stir zone *C* of M-FSP using traditional way; (d) The second pass stir zone *F*; (e) The third pass stir zone *H*; (f) Transitional zone *G* between second and third pass of M-FSP using novel way

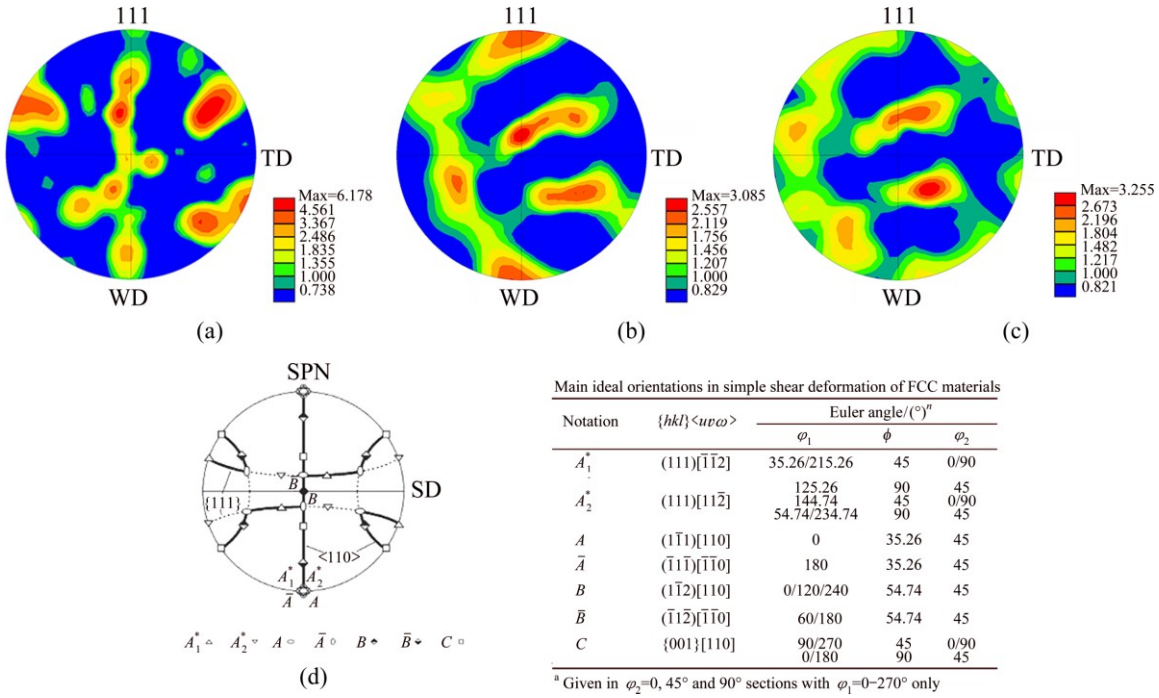

Main ideal orientations in simple shear deformation of FCC materials

Notation	{*hkl*}<*uvw*>	Euler angle/(°)[a]		
		φ_1	ϕ	φ_2
A_1^*	(111)[$\bar{1}\bar{1}$2]	35.26/215.26	45	0/90
A_2^*	(111)[11$\bar{2}$]	125.26 144.74 54.74/234.74	90 45 90	45 0/90 45
A	($\bar{1}$1$\bar{1}$)[110]	0	35.26	45
$\bar{A}$	($\bar{1}$1$\bar{1}$)[$\bar{1}\bar{1}$0]	180	35.26	45
B	($\bar{1}$1$\bar{2}$)[110]	0/120/240	54.74	45
$\bar{B}$	($\bar{1}$1$\bar{2}$)[$\bar{1}\bar{1}$0]	60/180	54.74	45
C	{001}[110]	90/270 0/180	45 90	0/90 45

[a] Given in φ_2=0, 45° and 90° sections with φ_1=0−270° only

Fig. 4 (111) pole figures showing texture in transitional zone *G* (between the 2nd and 3rd passes) before (a) and after (b) the third pass conducted, SZ of single-pass FSP (c) and main ideal simple shear components for FCC metals for comparison (d)

back during the previous pass. After the previous pass, as shown in Fig. 5, the volume fractions of the LAGBs and the subgrains in the transitional zone are relative high. This indicates that, despite the lack of stirring of the pin, the dynamic recovery (DRV) happens because of the insufficient strain imposed by the shoulder, and the grain

structure consists of subgrains. When the subsequent pass is conducted, the material of the previous pass is on the advanced side, and the flow direction is reversed. Dislocations are continuously generated in grains and subgrains, and the DRX on the basis of the DRV happens. The opposite flow direction accumulated the strain, leading to a gradual grain refinement in the transitional zone (Fig. 3(e)).

Besides the grain size, the morphology of the strengthening precipitates are observed by TEM, and the micrographs of the strengthening precipitates in locations *A*, *C*, *F*, *H*, *G* and the base metal are presented in Fig. 6. The morphology of the precipitates varies depending on both the moving distance and the order of FSP pass. For the traditional way, fine precipitates in the 3rd pass stir zone (Fig. 6(a)) disperse uniformly throughout the matrix. These fine precipitates are the strengthening phase $MgZn_2$ which have broken, dissolved and re-precipitated during FSP. However, the precipitates get coarsened and overaged in the previous pass stir zones (Fig. 6(b)), which is caused by the FSP thermal cycles of the subsequent passes [20]. For the novel way, the precipitates keep fine in the respective stir zone (Figs. 6(c) and (d)), and it seems that the overaging in the previous pass stir zone is inhibited due to the larger moving distance. Differently, the transitional zone is full of coarse precipitates (Fig. 6(e)) which are similar to those in the base metal (Fig. 6(f)), and no fine precipitates are observed.

3.2 Mechanical characteristics of processed zone

Figure 7 shows the hardness profile of M-FSP samples with different moving distances. The hardness of the single-pass FSP sample is also included for comparison (Fig. 7(a)). The processed zones produced by both single- and multi-pass FSP are strengthened compared with that of the base metal, the elevation in hardness is no less than HV 40. For the traditional way (Fig. 7(b)), compared with the hardness of the 3rd pass region, the hardness of the 1st and 2nd pass regions is

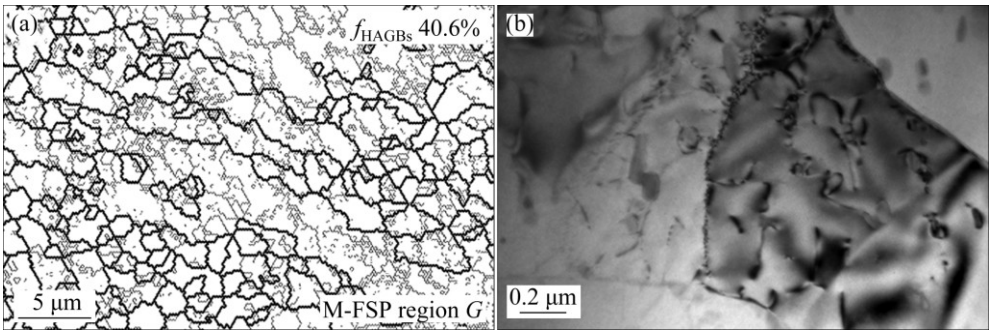

Fig. 5 EBSD grain-boundary map (a) and TEM image (b) in transitional zone *G* (between the 2nd and 3rd passes) before the third pass conducted

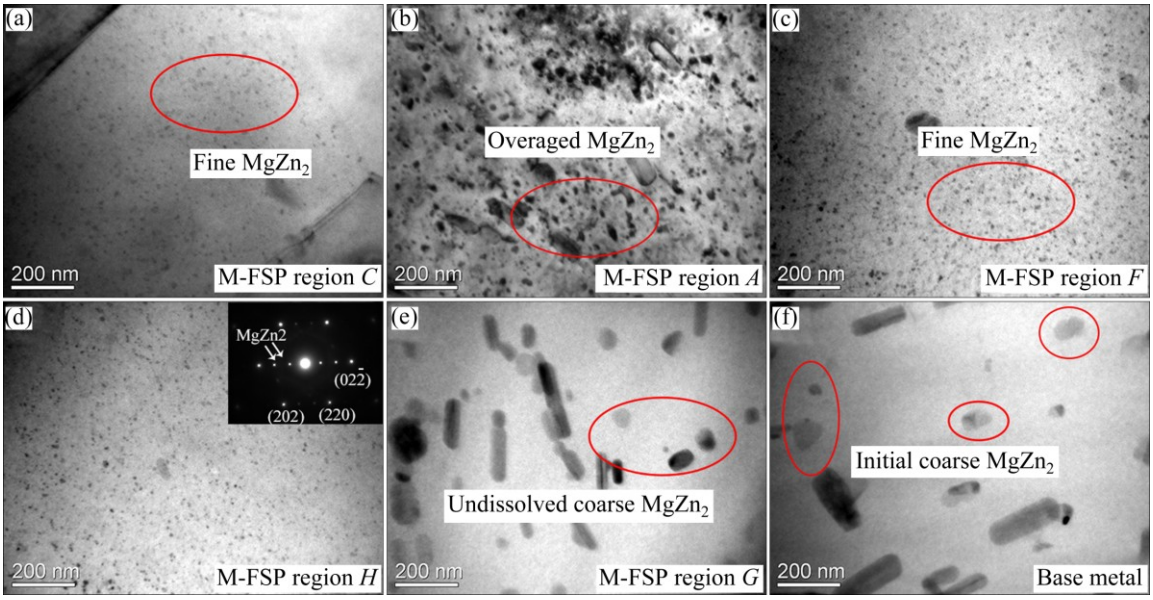

Fig. 6 TEM images taken from different regions in the 3rd pass stir zone *C* (a) and the 1st pass stir zone *A* of M-FSP using traditional way (b), the second pass stir zone *F* (c), and the third pass stir zone *H* (d) and transitional zone *G* between the 2nd and 3rd pass of M-FSP using novel way (e), and base metal (f)

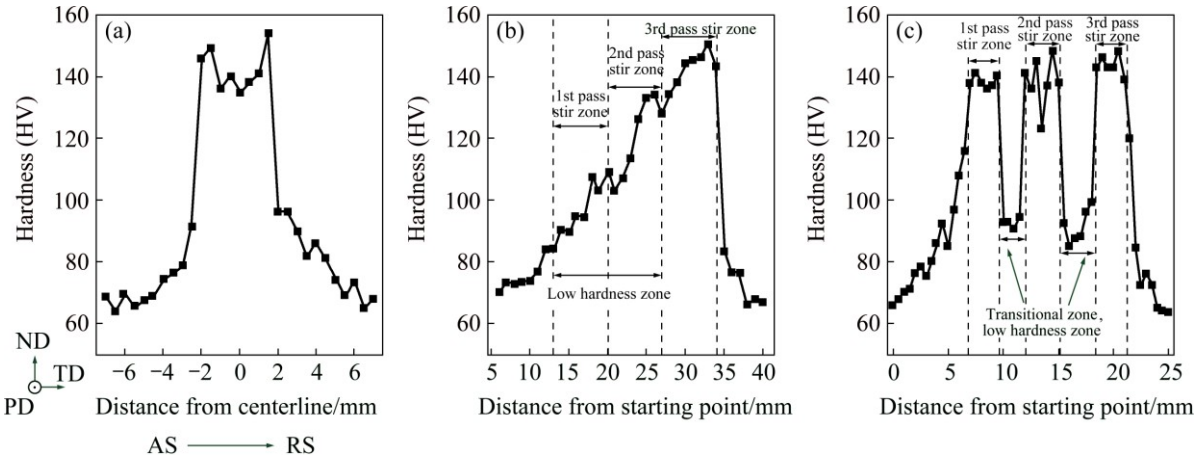

Fig. 7 Hardness profiles measured across processed zone of single-pass FSP (a), M-FSP using traditional way (b) and novel way (c) at 400 r/min rotational speed

much lower, and the width of this weak region is more than 6 mm. The hardness of the 3rd pass stir zone is similar to that achieved in the single-pass FSP sample. For the novel way (Fig. 7(c)), the hardness in the processed zone presents periodicity, the hardness of the 1st−3rd pass stir zones keeps the same level as that of single-pass FSP sample, the weak region locates in the transitional zone, and this weak region between the adjacent passes is about 2 mm. Table 3 shows the tensile strength of base metal, single- and multi-pass FSP samples. On one hand, the FSP-processed zones are strengthened by both single- and multi-pass FSP compared with the base metal, which is attributed to the fine grain microstructure in the processed zone as grain refinement is an effective way to improve the strength of materials [21]. On the other hand, all the M-FSP samples are failed in the weak region, and the tensile strength of M-FSP samples decreases compared with single-pass FSP sample on account of the existence of these regions.

Table 3 Tensile properties of base metal, single-pass and M-FSP samples

Processing condition	Ultimate tensile strength/MPa	Yield strength/MPa	Fracture location
Base metal	215±0	110±2	−
Single-pass FSP	323±3	223±1	−
3-pass FSP (traditional)	295±1	185±2	1st pass stir zone
3-pass FSP (novel)	305±2	213±3	1st−2nd pass transitional zone

Based on our previous studies [17,22], for precipitation-hardened aluminum alloys, besides the grain refinement, the mechanical properties are also affected by precipitation strengthening, and the mechanical properties will deteriorate due to the occurrence of the coarse precipitates. Therefore, the weak region in the processed zone is related to the distribution of the coarse precipitates, as shown in Figs. 6(b) and (e). The originating mechanisms of the low hardness zone in the traditional and novel way are investigated. As to the annealed 7B04 Al, the initial precipitates in the base metal are coarse and the dissolution behavior of these precipitates during FSP is relatively negative (Fig. 6(f)), and these coarse precipitates are difficult to dissolve during FSP when the heat input is insufficient [17]. For the traditional way, each stir zone undergoes no less than one time direct stirring by the pin with a relative high heat input, and the grains in the stir zone get refined and the precipitates dissolve during FSP. Subsequently, the precipitates reform and get coarsened during the following heating periods, decreasing the hardness and tensile strength of the previous pass stir zone, thus the weak region in the traditional way is mainly caused by the reformed overaged precipitates. For the novel way, the strain caused by the shoulder in the transitional zone is enough for inducing grain refinement. However, the transitional zone locates away from the stir zone, and the heat input here is much lower than that of the stir zone [23]. On account of the insufficient heat input, the dissolution of the precipitates in the transitional zone is inhibited, and most of the precipitates remain and keep coarse. Therefore, the weak region in the novel way is caused by the existence of these undissolved coarse precipitates.

3.3 Further investigation by applying higher rotational speed

The weak region is undesired for M-FSP, and hence it is necessary to narrow the width of this region. A higher rotational speed of 1000 r/min with the same travel speed of 200 mm/min was also adopted in the

present work, then the hardness profiles of the traditional and novel way are measured (Fig. 8). For the traditional way, the overaging of the previous pass is not avoided, meanwhile, the low hardness zone broadens from 6 to 8.5 mm. This is because the higher rotational speed aggravates the thermal cycle during FSP and increases the level of overaging in the previous pass. On the contrary, the weak region in the novel way is narrowed, which decreases from 2 to less than 0.5 mm. High heat input may lead to intense dissolution of coarse precipitates in the transitional zone, increasing the hardness and narrowing the weak region. In conclusion, it can be deduced that the weak region can be narrowed effectively by applying high rotational speed.

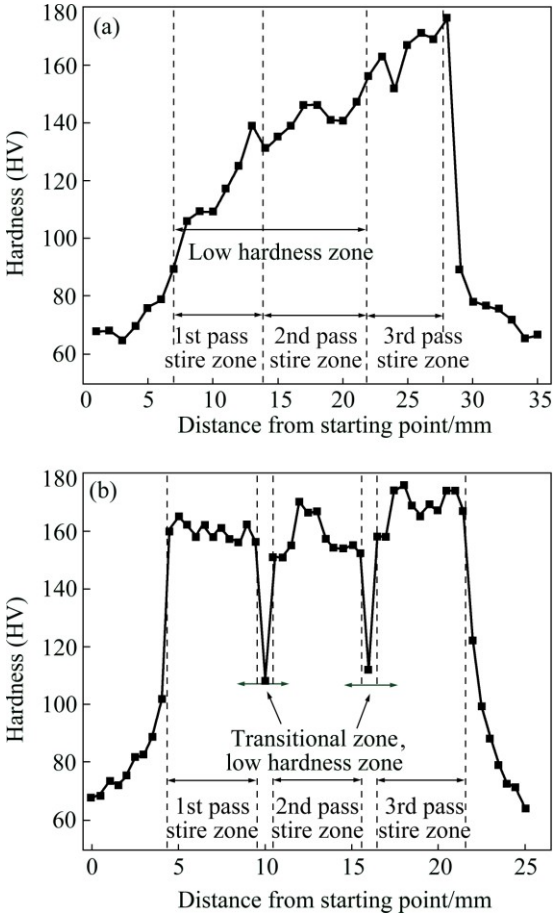

Fig. 8 Hardness profiles measured across processed zone of M-FSP using traditional (a) and novel (b) way with rotational speed of 1000 r/min

4 Conclusions

1) M-FSP was an effective method to produce fine-grained 7B04-O Al alloy, and the grain size was independent of the moving distance. The location of the weak region in the processed zone varied depending on the moving distance, where it was the previous pass stir zone in the traditional way and transitional zone in the novel way.

2) The weak region of traditional way was caused by the overaged microstructure, and the overaging could not be avoided associated with the intense thermal cycles during M-FSP. Differently, the weak region of the novel way was arisen from the undissolved coarse precipitates, and the weak region could be narrowed with increasing the rotational speed.

Acknowledgements

The financial support received from the Ministry of Education and Science, Russia, (Belgorod State University project No.1533) is acknowledged. The authors are grateful to the personnels of the Joint Research Centre at Belgorod State University for their assistance with the instrumental analysis.

Besides, one of the authors (Zhi-hui CAI) gratefully acknowledges support from the National Science Foundation for Young Scientists of China (No. 51501035) and Chinese Postdoctoral Science Foundation (No. 2016T90227). This research is supported financially by the National Natural Science Foundation of China (No. 51334006).

References

[1] MISHRA R S, MAHONEY M W, MCFADDEN S X, MARA N A, MUKHERJEEL A K. High strain rate superplasticity in a friction stir processed 7075 Al alloy [J]. Scripta Materialia, 1999, 42(2): 163−168.

[2] MA Z Y, MISHRA R S, MAHONEY M W. Superplastic deformation behavior of friction stir processed 7075Al alloy [J]. Acta Materialia, 2002, 50(17): 4419−4430.

[3] MA Z Y, MISHRA R S. Development of ultrafine-grained microstructure and low temperature ($0.48T_m$) superplasticity in friction stir processed Al−Mg−Zr [J]. Scripta Materialia, 2005, 53(3): 75−80.

[4] LIU F C, MA Z Y. Achieving exceptionally high superplasticity at high strain rates in a micrograined Al−Mg−Sc alloy produced by friction stir processing [J]. Scripta Materialia, 2008, 59(8): 882−885.

[5] CHEN Y, DING H, LI J Z, CAI Z H, ZHAO J W, YANG W J. Influence of multi-pass friction stir processing on the microstructure and mechanical properties of Al-5083 alloy [J]. Materials Science and Engineering A, 2016, 650: 281−289.

[6] SU J Q, NELSON T W, STERLING C J. Friction stir processing of large-area bulk UFG aluminum alloys [J]. Scripta Materialia, 2005, 52(2): 135−140.

[7] LIU F C, MA Z Y. Contribution of grain boundary sliding in low-temperature superplasticity of ultrafine-grained aluminum alloys [J]. Scripta Materialia, 2010, 62(3): 125−128.

[8] RAMESH K N, PRADEEP S, PANCHOLI V. Multipass friction-stir processing and its effect on mechanical properties of aluminum alloy 5086 [J]. Metallurgical and Materials Transactions A, 2012, 43(11): 4311−4319.

[9] JOHANNES L B, MISHRA R S. Enhanced superplasticity through friction stir processing in continuous cast AA5083 aluminum [J]. Materials Science and Engineering A, 2007, 464(1−2): 255−260.

[10] XUE P, XIAO B L, MA Z Y, Achieving large-area bulk ultrafine grained Cu via submerged multiple-pass friction stir processing [J]. Journal of Materials Science, 2013, 29(12): 1111−1115.

[11] ZHAO Y, DING Z, SHEN C, CHEN Y. Interfacial microstructure and properties of aluminum magnesium AZ31B multi-pass friction stir processed composite plate [J]. Materials & Design, 2016, 94: 240−252.
[12] JOHAANES L B, MISHRA R S. Multiple passes of friction stir processing for the creation of superplastic 7075 aluminum [J]. Materials Science and Engineering A, 2007, 464(1−2): 255−260.
[13] EL-RAYES M M, EL-DANAF E A. The influence of multi-pass friction stir processing on the microstructure and mechanical properties of aluminum alloy [J]. Journal of Materials Processing Technology, 2012, 212: 1157−1168.
[14] AL-FADHALAH K J, ALMAZROUEE A I, ALORAIER A S. Microstructure and mechanical properties of multi-pass friction stir processed aluminum alloy 6063 [J]. Materials & Design, 2014, 53: 550−560.
[15] HU Z , YUAN S, WANG X, LIU G, HUANG Y. Effect of post-weld heat treatment on the microstructure and plastic deformation behavior of friction stir welded 2024 [J]. Materials & Design, 2011, 32: 5055−5060.
[16] ZHAO Y Q, LIU H J, CHEN S X, LIN Z, HOU J C. Effects of sleeve plunge depth on microstructures and mechanical properties of friction spot welded alclad 7B04-T74 aluminum alloy [J]. Materials & Design, 2014, 62: 40−46.
[17] CHEN Y, DING H, CAI Z H, ZHAO J W, LI J Z. Effect of initial base metal temper on microstructure and mechanical properties of friction stir processed Al-7B04 alloy [J]. Materials Science and Engineering A, 2016, 650: 396−403.
[18] MISHRA R S, MA Z Y. Friction stir welding and processing [J]. Materials Science and Engineering R, 2005, 50: 1−78.
[19] FENG X L, LIU H J, BABU S S. Effect of grain size refinement and precipitation reactions on strengthening in friction stir processed Al−Cu alloys [J]. Scripta Materialia, 2011, 65(12): 1057−1060.
[20] MA Z Y, SHARMA S R, MISHRA R S. Effect of multiple-pass friction stir processing on microstructure and tensile properties of a cast aluminum-silicon alloy [J]. Scripta Materialia, 2006, 54(9): 1623−1626.
[21] SATO Y S, KOKAWA H, ENOMOTO M, JOGAN S, T. HASHIMOTO T. Precipitation sequence in friction stir weld of 6063 aluminum during aging [J]. Metallurgical and Materials Transactions A, 1999, 30: 3125−3130.
[22] CHEN Yu, DING Hua, LI Ji-zhong, ZHAO Jing-wei, FU Ming-jie, LI Xiao-hua. Effect of welding heat input and post-welded heat treatment on hardness of stir zone for friction stir-welded 2024-T3 aluminum alloy [J]. Transactions of Nonferrous Metals Society of China, 2015, 25: 2524−2532.
[23] NANDAN R, DEBROY T, BHADESHIA H K D H. Recent advances in friction-stir welding-Process, weldment structure and properties [J]. Progress in Materials Science, 2008, 53(6): 980−1023.

多道次搅拌摩擦加工对 7B04-O 铝合金组织和性能的影响

陈 雨[1]，丁 桦[1]，S. MALOPHEYEV[2], R. KAIBYSHEV[2]，蔡志辉[1]，杨文静[1]

1. 东北大学 材料科学与工程学院，沈阳 110819；
2. Laboratory of Mechanical Properties of Nanoscale Materials and Superalloys, Belgorod State University, Belgorod 308015, Russia

摘 要：采用不同的相邻道次搅拌头位移量对 7B04-O 铝合金进行三道次搅拌摩擦加工，相邻道次的搅拌头位移量分别采用传统方式(50%搅拌针直径)和新方式(50%搅拌轴肩直径)。搅拌摩擦加工引起晶粒和第二相粒子细化，加工区力学性能提高，硬度提高 HV40，拉伸性能也较母材提高了 40%。在加工区内部存在性能弱区，其位置受相邻道次搅拌头位移量影响，当采用传统方式的搅拌头位移量时，性能弱区为先前加工道次，而采用新方式时，性能弱区为过渡区。利用新方式制备细晶加工区时，可以通过提高搅拌头旋转速度限制性能弱区。

关键词：搅拌摩擦加工；多道次；晶粒细化；铝合金

(Edited by Xiang-qun LI)